Prediction of the aeroacoustic noise of a radial fan using Lighthill's Analogy in frequency domain

Hakan Dogan[1], Martin Ochmann[1], Chris Eisenmenger[2], Stefan Frank[2]

[1] *Beuth Hochschule für Technik, 13353 Berlin, E-Mail:hdogan, ochmann@beuth-hochschule.de*

[2] *Hochschule für Technik und Wirtschaft, 12459 Berlin, E-Mail: c.eisenmenger, stefan.frank@htw-berlin.de*

Introduction

Radial fans are used in many important engineering applications such as automotive, heating or cooling. In this study, the aerodynamic and acoustic performance of a radial fan used in household laundry dryers is investigated. Regarding the design criteria, it is desired to increase the efficiency of the fan and to reduce the aeroacoustic noise [1, 2]. It is well-known that the fans with backward curved blades provide higher efficiency, however with the drawback of a louder tonal noise at the blade passing frequency. The geometrical and the aerodynamic performance details of a reference radial fan with nine backward blades were presented in publications [1] and [2] by the current authors. Although some ongoing work focuses on the optimization of the blade profiles, the aeroacoustic results in the current article will be based on the reference fan, which is detailed in Refs. [1] and [2].

In terms of numerical simulations, the usual CFD/CAA (computational fluid dynamics/computational aeroacoustics) approach is employed here. In the CFD simulations, the near field variables (pressure and velocity correlations) are computed with ANSYS-CFX software [3]. In particular, the Stress-Blended Eddy Simulation (SBES) approach based on the Shear Stress Turbulence (SST) model is used in CFD computations.

Several aeroacoustic wave formulations and analogies have been proposed in the literature, e.g. Lighthill's formulation [4], Curl's analogy [5], or Ffowcs Williams – Hawkings equation etc. These formulations have discussed the effects of the monopole, dipole and quadrupole sound sources in relation to the problem being solved. In the current paper, we perform aeroacoustic simulations based on the integral form of Lighthill's equation [4] and investigate, in particular, the effects of the quadrupole sources on the overall noise spectrum. The far field acoustic pressure is evaluated using the direct boundary element method (DBEM).

Integral forms of the wave equations have been widely applied in computational aeroacoustics. Lyrintzis [6] presented a review explaining the details of the well-known Lighthill's analogy, Kirchhoff formulation and the Ffowcs Williams - Hawkings equation. Integral equations have the specific advantage of involving the first or second order derivatives of the (analytical) test function, instead of the numerical derivatives of the corresponding field variables. As a result, more accurate noise predictions can be performed. Schram [5] has presented a boundary element extension of Curle's analogy for non-compact geometries. In Ref. [5], monopolar, dipolar and quadrupolar noise contributions from the spinning of a vortex pair in an infinite two-dimensional duct were investigated in detail, which is particularly relevant to the problem in the current paper.

Experimental setup

The aeroacoustic measurements were performed using a test rig (the so-called In-Duct method) according to the industry norm ISO 5136 [7], installed at HTW Berlin. The far-field noise levels are recorded inside a circular duct using three slit-tube microphones (see Fig. 1).

The measurements were done with a duration of 35 seconds at each of the three microphones and were repeated 10 times. The recorded signals were post-processed with Samurai software from Sinus Acoustics. The Fourier transform of the signals were taken and averaged over all samples and microphones. Moreover, corrections due to the flow velocity and the shield protection of the microphones were done according to the formulas in Ref. [7]. The experimental results presented in the current paper have a frequency resolution of ~12 Hz.

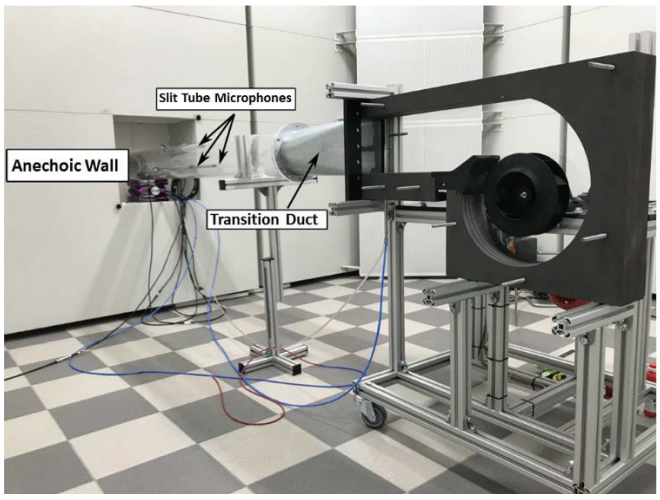

Figure 1: The experiment setup in the semi anechoic room at HTW Berlin (After Ref. [1]).

Computational Fluid Dynamics

The CFD mesh consisted of approximately 30-35 million nodes with mainly tetrahedral elements. Moreover, 15-20 prism layers were created near the solid walls in order to resolve the boundary layers.

One of the primary aims of the CFD simulations is to calculate the static efficiency (η_{st}) of the fan, which is given by

$$\eta_{\mathrm{st}} = \frac{\dot{V}\,\Delta p_{\mathrm{st}}}{M\,2\pi n} \tag{1}$$

where $\dot{V}$ is the volumetric flow rate, Δp_{st} is the static pressure rise, n is the rotational speed and M is the total torque acting on the rotor.

The simulations were run for 8 revolutions of the rotor, where a converged steady solution was used as the initial condition. Hence, the last 4-6 revolutions of the simulations provided reliable time-dependent data. In Ref. [2], the instantaneous aerodynamic pressure on the blades of the fan during a simulation were shown.

Computational Aeroacoustics

Lighthill's equation for aeroacoustic wave propagation is given in frequency domain as [8]

$$\nabla^2 p + k^2 p = \nabla \cdot \left(\nabla \cdot \tilde{T}_{ij}\right), \tag{2}$$

where k is the wavenumber and $\tilde{T}_{ij}$ is the Fourier transform of Lighthill tensor T_{ij}, which is given for low Mach number flows as

$$T_{ij} = \rho v_i v_j. \tag{3}$$

In Eq. (3), ρ is the density and v_i are the components of the velocity.

Let us denote the boundary enclosing the acoustic domain as $\Gamma = \Gamma_{\mathrm{I}} \cup \Gamma_{\mathrm{w}} \cup \Gamma_{\mathrm{o}}$, where Γ_{I} is the permeable surface (the inlet), Γ_{o} is the circular outlet of the duct, and Γ_{w} is the rigid side walls between the inlet and outlet. The acoustic pressure $p(x_i)$ at an internal point x_i within the domain can be obtained using the following integral equation [5]:

$$p(y_i) = \int_{V_q} dV\ \tilde{T}_{ij} \frac{\partial^2 G(x,y)}{\partial x_i\,\partial x_j} + \int_{\Gamma} G \frac{\partial p}{\partial n} - p \frac{\partial G}{\partial n} d\Gamma, \tag{4}$$

where the Green's function G is given by

$$G = \frac{e^{-ikr}}{4\pi r}. \tag{5}$$

In Eq. (5), r is the distance between the collocation point y_i and the integration points on the surface Γ and in the volume V. In order to complete the above defined problem, the boundary conditions should be prescribed. At the permeable interface Γ_{I}, the acoustic pressure is prescribed by taking the Fourier transform of the time-domain pressure values (p_t) obtained in the CFD simulations:

$$p(\boldsymbol{x},\omega) = \int_{-\infty}^{\infty} p_t(\boldsymbol{x})\, e^{-i\omega t}\ dt, \qquad \boldsymbol{x} \in \Gamma_{\mathrm{I}}. \tag{6}$$

On the rigid side walls, the particle velocity is zero. Therefore, the hard-wall condition is employed, i.e.

$$\frac{\partial p(\boldsymbol{x})}{\partial n} = 0 \qquad \boldsymbol{x} \in \Gamma_{\mathrm{w}}. \tag{7}$$

At the outlet, the plane-wave impedance condition is prescribed:

$$Z(\boldsymbol{x}) = \rho\, c \qquad \boldsymbol{x} \in \Gamma_{\mathrm{o}}, \tag{8}$$

where c is the speed of sound.

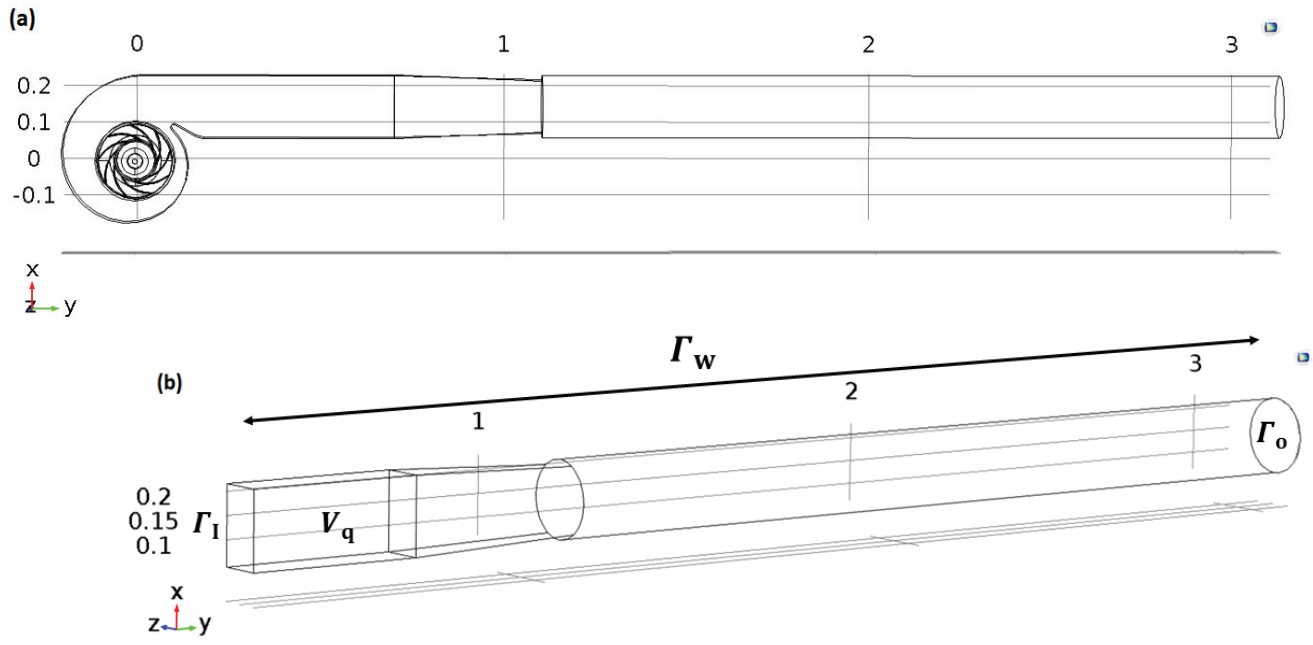

Figure 2: (a) The CAD file of the experimental setup, and (b) the acoustic calculation domain for Configuration 1.

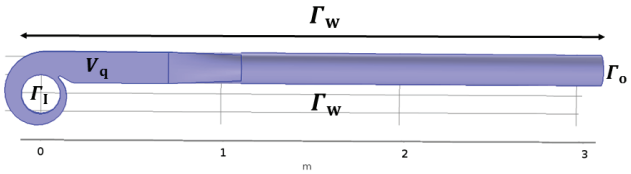

Figure 3: Acoustic calculation domain with the cylindrical interface (Configuration 2).

For the CAA domain, we set two different configurations: In Configuration 1, the pressure data from CFD is taken at a rectangular plane y=0.2 m (see Fig. 2b). In this case, the volume V_q where the quadrupole sources are integrated lies between y=0.2 m and y=0.7 m planes. In Configuration 2, the CFD pressure data is taken at the virtual cylindrical interface outside the rotor (see Fig. 3). In this case, the domain for the quadrupole sources (V_q) is the volume between the cylindrical interface and y=0.7 m plane. In both configurations, we calculate the acoustic pressure p_q in the midpoint of y=0.7m plane. In Ref [9], it was shown that in the region y>0.7 m the acoustic waves propagate as plane waves below the cut-off frequency. Therefore, the acoustic pressure p_{ac_m} at the location of the microphones can be calculated analytically as

$$p_{ac\_m} = p_q \, e^{-ik(y_m - y_I)}, \qquad (9)$$

where $y_m = 2.47$ m is the y-coordinate of the microphones, and y_I is the y-coordinate of the end of near field (CFD) domain, e.g. $y_I = 0.7$ m.

The set of equations (4) - (8) is solved using the in-house developed direct boundary element method, which is a modified version of the algorithm in Ref. [10]. For the numerical discretization, constant boundary elements with an edge length of maximum 0.010 m are used.

Although integral equation based simulations are performed in this article, the quantitative and qualitative visualisation of the quadrupole sources on the right hand side of Eq. (2) can be presented in the near field. For instance, Fig. 4 shows the magnitude of the variable $\nabla \cdot (\nabla \cdot \tilde{T}_{ij})$ in frequency domain at the BPF (429 Hz). A video file for the time domain evolution can be found at the web-link [11].

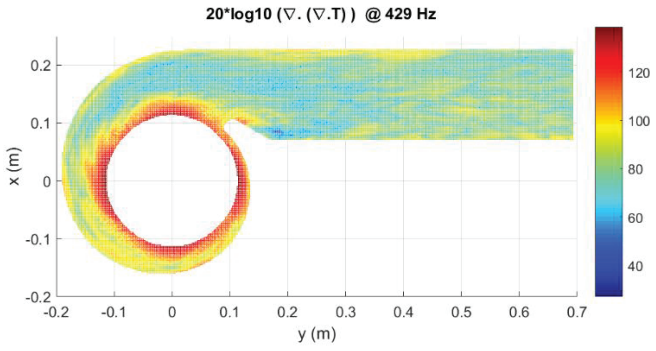

Figure 4: Frequency domain distribution of the acoustic quadrupoles at the BPF.

Results

The results of the aeroacoustic simulations using Eq. (4) are presented in this section. The pressure fluctuations and the velocity correlations in the CFD simulations are computed on a grid which is considerably finer than the acoustic grid. Therefore, we interpolate the values of these variables onto the acoustic grid. For the data interpolation, the radial basis functions (RBFs) are used. In the RBF approximation, the nearest neighbouring nodes (e.g. 20 nodes) in the fine grid are determined for each node in the coarse grid.

In Fig. 5, the numerical values for the acoustic pressure obtained using the BEM at the microphone location are shown for CAA domain Configuration 1. The results with and without including the quadrupole effects are shown. The solid black line shows the results with quadrupole sources and the red line shows the experiment result. The blue dashed line shows the noise spectrum without the volumes sources, i.e. without the volume integral in Eq. (4). It can be seen that the addition of such sources improve the results at some discrete frequencies at the low frequency range. The quadrupole sources have no considerable impact above ~600 Hz. For the considered experimental test rig and the geometry, the outlet duct has a cut-off frequency of ~1170 Hz [4]. The numerical and experimental results agree well at the BPF, indicating a sound pressure level (SPL) of ~86 decibels.

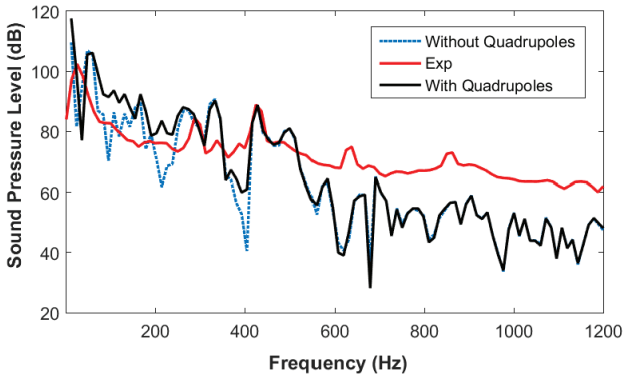

Figure 5: Results of the simulation for the Configuration 1, in which the virtual interface is located at y=0.2m.

In Fig. 6, the numerical results for the acoustic pressure for Configuration 2 are presented, and compared with the experimental data. The black line shows the sound spectrum with quadrupoles, the blue line shows the spectrum without quadrupoles and the red line presents the experimental data. As can be seen, quadrupole sources are effective at low and mid frequencies, i.e. up to ~700 Hz. The SPLs between the numerical and the experimental results agree considerably well.

The numerical results presented here have a frequency resolution of ~12 Hz, which corresponded to the time domain CFD results for four revolutions of the radial fan. Through ongoing work, the time domain length of the unsteady CFD simulations has been extended to eight rotations of the fan. This will enable us to perform frequency

domain simulations with a frequency step of 6 Hz. Alternatively, the power spectral density results can be calculated.

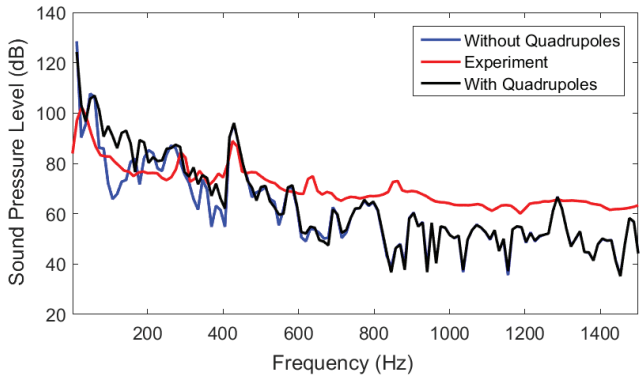

Figure 6: Results of the simulation where the virtual interface is selected as the cylindrical interface (Configuration 2).

Conclusions

In this work, the aerodynamic and the aeroacoustic characteristics of a radial fan is investigated. A backward curved fan with nine blades and a diameter of 200 mm has been designed and prototyped. For the near field simulations, SBES-SST based CFD computations have been performed in order to determine the aerodynamic characteristics. The computational aeroacoustics approach is based on applying the integral form of Lighthill's equation to determine the acoustic pressure at the end of the near field region. Within the outlet duct, the acoustic waves propagate as plane waves. Two different choices have been used for the CAA domain. Accordingly, the permeable interface in the near field has been taken either as the cylindrical surface outside the rotor, or as the rectangular surface after the volute tongue (at y=0.2m).

The comparisons between the experimental data and the numerical simulations have shown good agreement. In particular, the impact of the quadrupole sources on the overall sound spectra has been observed rather at the low-to-mid frequency range, e.g. below 600 Hz. Further refinements will be performed in order to improve the design parameters such as efficiency and radiated sound power levels.

Acknowledgements

The authors are thankful to the BMBF and the project partners ANSYS, B/S/H/ and GRONBACH for their support.

GEFÖRDERT VOM
Bundesministerium für Bildung und Forschung

FORSCHUNG AN FACHHOCHSCHULEN

References

[1] C. Eisenmenger, S. Frank, H. Dogan, M. Ochmann: Aerodynamische und aeroakustische Untersuchungen an Radialventilatoren mit rückwarts gekrümmten Schaufeln für Haushaltsgeräte. Proc. 44. Jahrestagung für Akustik - DAGA (2018) 1208-1211.

[2] C. Eisenmenger, S. Frank, H. Dogan, M. Ochmann: High Efficiency Low Noise Heatpump Dryer (HELNoise). Proc. 43. Jahrestagung für Akustik-DAGA (2017) 1491-1494.

[3] ANSYS – CFX, URL: http://www.ansys.com/Products/Fluids/ANSYS-CFX

[4] M. J. Lighthill: On sound generated aerodynamically. I. General Theory. Proc. R. Soc. Lond. A (211) (1952), 564-587.

[5] C. Schram: A boundary element extension of Curle's analogy for non-compact geometries at low Mach numbers. Journal of Sound and Vibration (322) (2009) 264-281.

[6] A. S. Lyrintzis: Surface integral methods in computational aeroacoustics – From the (CFD) near field to the (Acoustic) far field. International Journal of Aeroacoustics 2(2) (2003), 95-128

[7] Industrial Organization for Standardization, ISO 5136: Acoustics – Determination of sound power radiated into a duct by fans and other air-moving devices (2003) London

[8] C. Bogey, C. Bailly, D. Juve: Numerical simulation of sound generated by vortex pairing in a mixing layer. AIAA Journal (38) (2000), 2210-2218.

[9] H. Dogan, M. Ochmann, C. Eisenmenger, S. Frank: Hybrid CFD/FEM calculations for the aeroacoustic noise radiated from a radial fan. Euronoise (2018) 297-302.

[10] H. Dogan, M. Ochmann, C. Eisenmenger, S. Frank: A hybrid CFD/BEM method for the calculation of aeroacoustic noise from a radial fan. Proc. 44. Jahrestagung für Akustik - DAGA (2018) 493-496.

[11] HELNOISE Project, URL: https://projekt.beuth-hochschule.de/?id=2824